OPEN ACCESS PRESS (OAP)

OpenAccessPress.com/Journal/JFOPA

Journal of Fundamental and Observational Physics and Astrophysics

ISJN: JFOPA

Volume 1 Issue 1 - 2025

ISSN: Registering

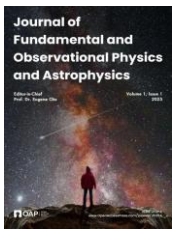

Research Article

Open Access

DOI: Registering

Carbon Swan Molecular Spectra Analyses

Christian G. Parigger [1,2]

1 CGP Consulting LLC, 361 Jack Thomas Drive, Manchester, TN 37355, USA; cgparigger@gmail.com

2 Former address: Physics and Astronomy Department, University of Tennessee, University of Tennessee Space Institute, Center for Laser Applications,
411 B.H. Goethert Parkway, Tullahoma, TN 37388-9700, USA

ABSTRACT: This article presents analysis of carbon Swan, C_2, laser-plasma emission records using line strength data, C_2-Swan-lsf, and the ExoMol astrophysical database. Line- strength data fitting of 0.25-nanometer spectral resolution ExoMol-computed spec- tra for a 6,000-Kelvin temperature C_2 Swan system, d $^3\Pi_g \longrightarrow$ a $^3\Pi_u$, $\Delta v = 0, \pm 1$, reveals a temperature of 5,640 Kelvin. The six per cent lower temperature is as- sociated primarily with the accuracy of the transition wavelengths in the ExoMol vs. C_2-Swan-lsf data. The analysis of experiment data examines spectra that are recorded following laser-induced optical breakdown in carbon monoxide. The laser plasma data are recorded with 0.35-nm spectral resolution. The temperature infer- ences are elaborated when using non-linear fitting with both databases. The results show temperatures in excess of 6,000 Kelvin for the $\Delta v = -1$ sequence, and for a time delay of 30 µs from laser plasma initiation. The accuracy of the C_2 Swan bands line strength data is of the order of 1 picometer. These line strength data are also utilized for analysis of laser-induced fluorescence experiments that employ a spectral resolution of 5.5 picometer, and a temperature of 2,716 Kelvin is inferred. Accurate C_2 databases show many applications in laboratory diagnosis and interpretation of astrophysical plasma records.

KEYWORDS: carbon Swan bands; laser-plasma; molecular spectroscopy; astrophysics

RECEIVED: 16 April 2025

ACCEPTED: 25 May 2025

PUBLISHED: 22 July 2025

ACADEMIC EDITOR(S): Eugene Oks

OPERATING EDITOR(S): Kumar Shrestha

REVIEWER(S): Eugene Oks

CITATION: Registering.

DOI: Registering.

1. Introduction

Swan bands are a characteristic of the spectra of carbon stars, comets, and burning hydrocarbon fuels. Swan bands consist of several sequences of vibrational bands scattered throughout the visible spectrum. Signatures of the diatomic carbon molecule, C_2, [1–3] occur in plasma-emission following the generation of laser-induced optical breakdown of carbon-containing materials, liquids, gases, including carbon monoxide gas [4]. Notable is of course, occurrence of C_2 Swan bands in combustion of hydrocarbons, emissions from white dwarf stars, e.g., Procyon B [5, 6], to name two specific examples. Usually, accurate diatomic line strengths data are preferred in the analysis [7–11] of recorded data. However, recent interest in exo-planet spectroscopy motivates determination of new molecular databases, viz. the ExoMol [12] database. The ExoMol database lists various C_2 isotopologues, however this work focuses on 12 C_2. The molecular transition of interest is the C_2 d $^3\Pi_g \longrightarrow$ a $^3\Pi_u$, $\Delta v = 0, \pm 1$ Swan band system [13].

Spectroscopy [13–19] of laser plasma reveals clean C_2 Swan bands for of several dozens of microseconds from the initial laser plasma generation using pulse widths of a few nanoseconds. For diatomic carbon spectroscopy, one can utilize the ExoMol or other databases in conjunction with the PGOPHER program [20, 21] for diatomic molecular spectroscopy. The ExoMol 12 C_2 data files for the states and the transitions are converted in this work to line strength files for the purpose of comparison with previously communicated and extensively tested C_2 [7–11] line-strength data that are conveniently accessed with MATLAB [22] scripts.

2. Experiment and Analysis Overview

The laser plasma experiment for recording of C_2 Swan bands comprises a standard laser- induced breakdown spectroscopy arrangement [4]. A Continuum YG680S-10 Nd:YAG device is operated at the fundamental IR wavelength of 1064 nm, 7.5 ns pulse width, 300 mJ energy per pulse, and a rate of 10 Hz. The laser beam is focused into a cell containing 99.97 % purity carbon monoxide with at most 0.02 % nitrogen gas impurity, at 22.4 kPa (3.25 psi) above atmospheric pressure. An optical multichannel analyzer manages electric gates and recordings of an intensified, 1024-pixels linear diode array mounted at the exit plane of a MonoSpec 27 Thermo Jarrel-Ash 0.275 monochromator. A 1800 grooves/mm holographic grating has a reciprocal linear dispersion of 2 nm/mm. Wavelength and sensitivity calibrations utile. Standard light pen-ray and tungsten light sources, respectively. Typically, averages over 200 individual laser-plasma events are accumulated with a gate width of 1 μs. The $\Delta v = -1$ sequence of the C_2 Swan system discussed in this work is recorded at a gate delay of 30 μs. Over and above the 1-μs average, the data represent a line-of-sight average of the expanding plasma.

The analysis of the diatomic molecular spectra utilizes line strength data, the Boltzmann equilibrium spectral program (BESP) and the Nelder-Mead downhill simplex, non-linear fitting algorithm [23] in conjunction with the Nelder-Mead temperature (NMT) program for computation and fitting of theory and experiment spectra. The molecular C_2 Swan line strengths "C_2-Swan-lsf" [8] are established using the Wigner-Witmer diatomic eigenfunctions [24, 25] and standard molecular spectroscopy methods [7]. In turn, the ExoMol states and transition files for C_2 [26, 27] are utilized for the generation of line strength data that can be used with BESP and NMT. The ExoMol data show Einstein A-coefficients that are converted to line strengths [28–31].

The C_2-Swan-lsf and ExoMol databases show vacuum wave numbers. In both BESP and NMT programs, air wavelengths are computed by including refractive index of air variations with wave number [32]. Details are elaborated in Refs. [8, 28]

including preference of considering Gaussian-profiles. Extensions to combined Lorentzian and Gaussian profiles, or Voigt profiles, can be implemented using standard spectroscopy approaches [33].

3. Results

This section elaborates diatomic molecular C_2 d $^3\Pi_g \longrightarrow$ a $^3\Pi_u$, $\Delta v = 0, \pm 1$ sequences and progressions. First, recorded spectra of the $\Delta v = -1$ sequence [4] are re-evaluated by fitting a linear, spectroscopically broad background and by minimizing the difference of theory and experiment spectra for the C_2-Swan-lsf data. Second, fitting of the recorded data is accomplished with ExoMol data that are transformed from Einstein A-coefficients to line strengths. Third, ExoMol C_2 data in the range of 440 − 590 nm are computed and then analyzed with C_2-Swan-lsf line strengths. Comparisons are included of laser induced fluorescence (LIF) data and C_2-Swan-lsf computed spectra in order to exhibit the accuracy of that theory data set. A separate LIF-program (not communicated here) is utilized because for LIF the wave numbers for the lower states of the transitions are needed [7].

Analysis of $\Delta v = -1$ Swan Spectra with NMT Program and C_2-Swan-lsf Line Strengths

A previous analysis of the $\Delta v = -1$ sequence [4] shows a temperature of 6,745 K and for a spectral resolution of 0.35 nm (11.5 cm−1) when assuming zero background contributions. Over and above clearly developed Swan spectra for a time delay of 30 μs from laser-plasma initiation, there are background contributions from other radiating species. This background radiation is modeled to vary linear with wavelength. The background contributions are com- puted simultaneously with fitting the spectra for temperature determination while keeping the same spectral resolution. The NMT script would allow one to also fit the spectral resolution in the fitting of theory with experiment data.

Figure 1 illustrates spectra determined from temperature fitting with constant Gaussian line-width, $\Delta\bar{\lambda}$. The simulated spectrum utilizes the C_2-Swan-lsf data in the experimental range 528 nm − 565 nm. Analysis of the measured data leads to a C_2 excitation temperature of T = 7, 360 K.

Analysis of $\Delta v = -1$ Swan Spectra with NMT Program and ExoMol C_2 Line Strengths

For the analysis with ExoMol C_2 data, the states and transition files for C_2 [26, 27] are collated in a table that is compatible with the NMT program, including conversion of Einstein A-coefficients to line strengths. Tables 1 and 2 reveal the number of lines that agree within specified wave number values and the number of transitions, respectively.

Table 1. Subset of the C_2 ExoMol data that agree within $\Delta\tilde{\nu}$ of 5,032 transitions in the C_2-Swan-lsf data in the range 528.36 − 564.85 nm (17,704 − 18,926 cm−1).

Database	$\Delta\tilde{\nu} < 0.05\,\mathrm{cm}^{-1}$	$\Delta\tilde{\nu} < 0.2\,\mathrm{cm}^{-1}$	$\Delta\tilde{\nu} < 0.5\,\mathrm{cm}^{-1}$	$\Delta\tilde{\nu} < 2.0\,\mathrm{cm}^{-1}$	$\Delta\tilde{\nu} < 10.0\,\mathrm{cm}^{-1}$
ExoMol C_2	1,147	2,215	2,980	4,073	4,789

Figure 2 illustrates spectra determined from temperature and linear background fitting with constant Gaussian line-width, $\Delta\bar{\lambda}$. The results indicate a temperature of T = 5, 740 K

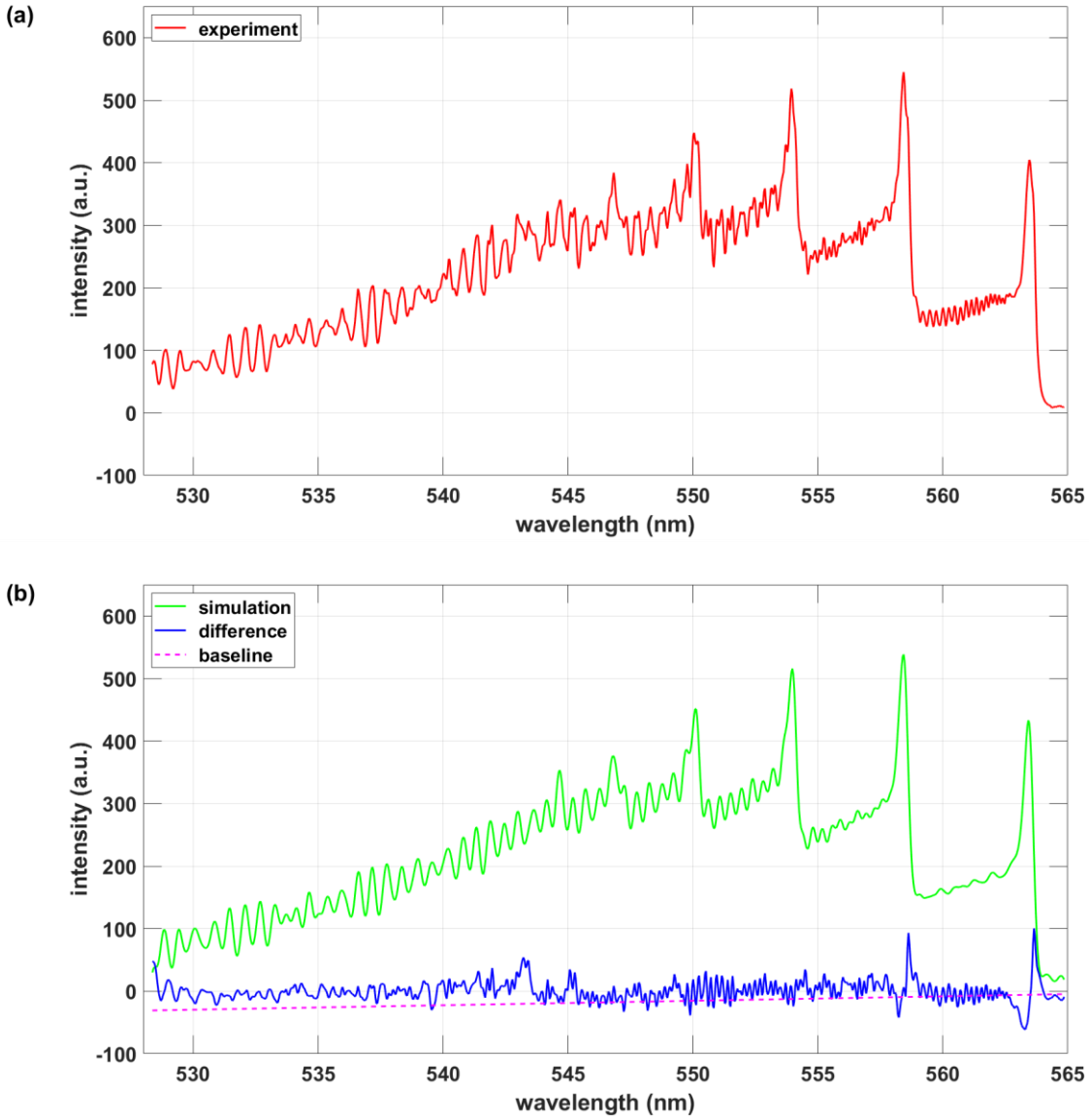

Figure 1. (a) Experiment. (b) NMT fitting with C_2-Swan-lsf data, T = 7, 360 K, fixed $\Delta^{-}\lambda = 0.35$ nm.

Table 2. Number of transitions in the range 528.36 − 565.85 nm (17,704 − 18,926 cm−1).

Database C_2 Swan 528 − 565 nm	**528 − 565 nm**	**Acoeff > $10^3 s^{-1}$**
ExoMol C_2	283,005	37,696
C_2-Swan-lsf	5,032	5,032

that is 1,890 K lower than that obtained with C_2-Swan-lsf fitting, see Fig. 1. The temperature discrepancy is attributed to the spectroscopically different line positions.

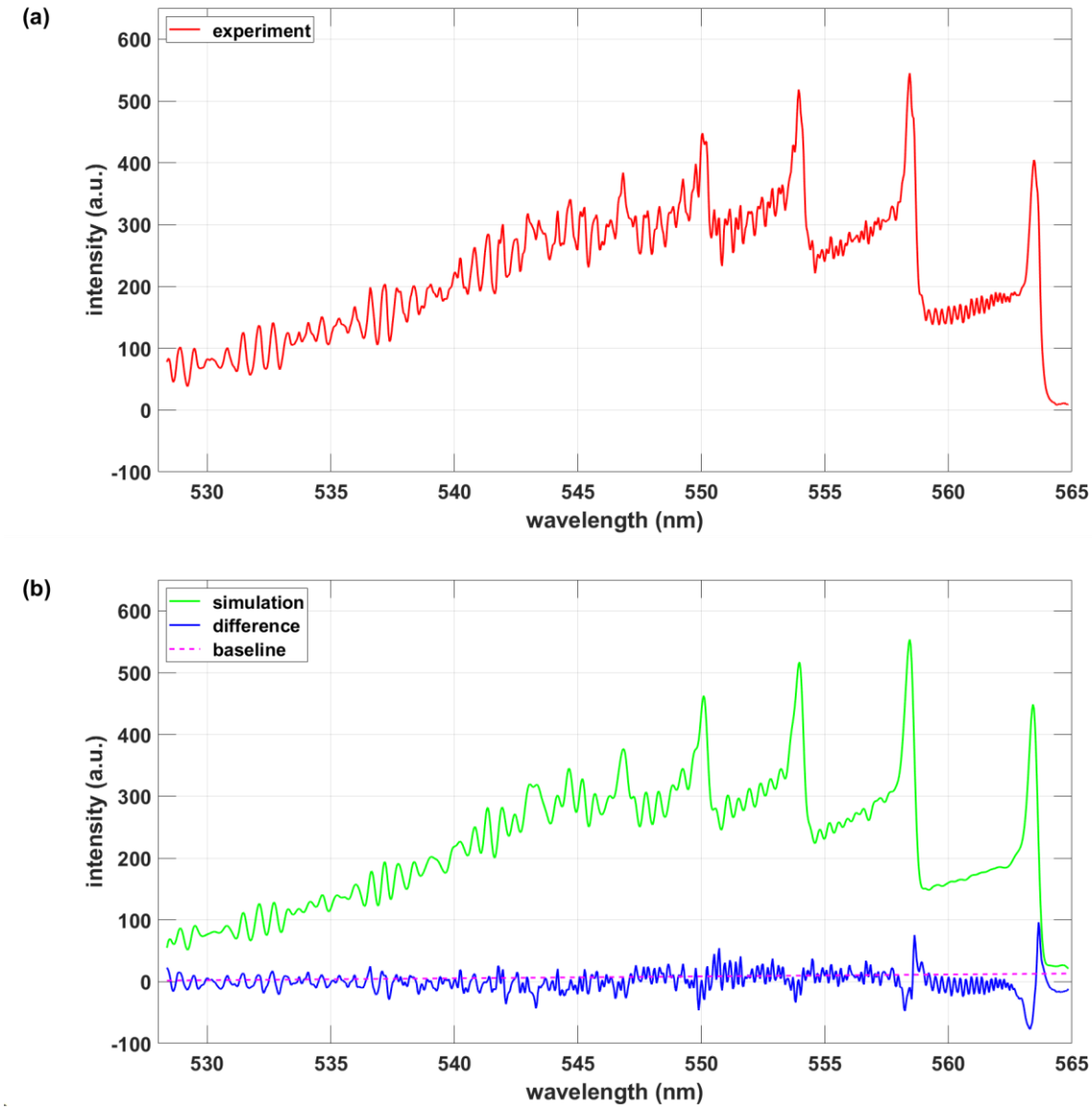

Figure 2. (a) Experiment. (b) NMT fitting with ExoMol C_2 data, T = 5, 740 K, fixed $\Delta\bar{\lambda} = 0.35$ nm.

The ExoMol C_2 data appear to successfully model in part the apparent differences near 543 nm in Figure 1 that suggest presence of so-called 6-7 high pressure band of C_2, a known intensity anomaly in the C_2 Swan system. However, subtle differences occur for the 2-3, 3-4, 4-5 bands near 554 nm, 550 nm, 547 nm, respectively. The 0-1 and 0-2 bands near 564 nm and 558 nm, respectively, reveal similar differences between experiment and theory spectra.

Swan Spectra $\Delta v = 0, \pm 1$: ExoMol C_2 and C_2-Swan-lsf Data Comparisons

Figure 3 illustrates ExoMol C_2 computed, or numerical experiment data, in the wave- length range 440 − 590 nm that are fitted using the NMT script and C_2-Swan-lsf data. The differences in temperature of 360 K can be associated with primarily the wave numbers that are listed in the ExoMol C_2 database. There may also be differences in the Frank-Condon factors and r-centroids, but this is not further evaluated in this work. Figure 3 (b) exhibits obvious differences near the heads of the various Swan bands.

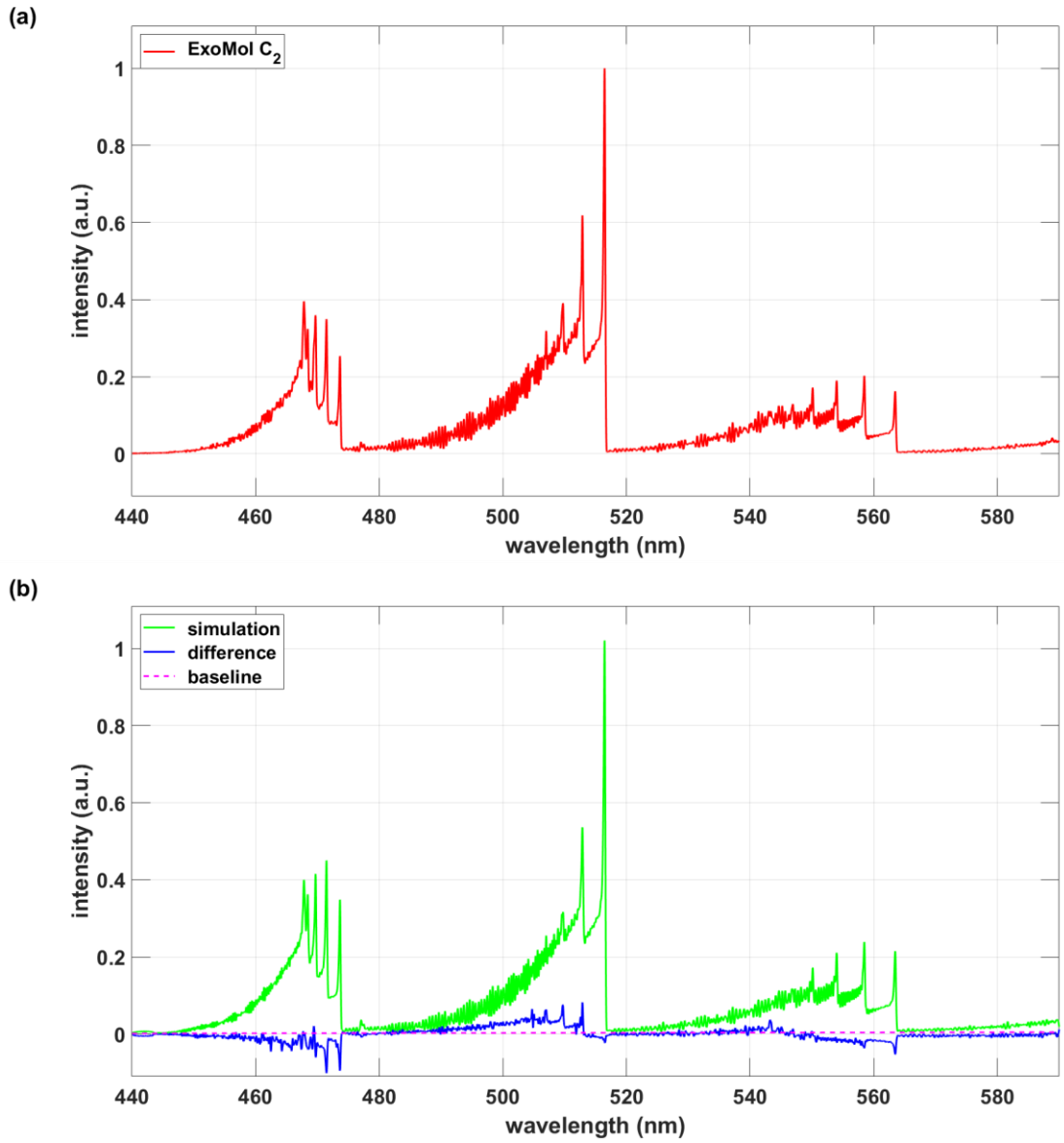

Figure 3. (a) Numerical experiment data, T = 6,000 K, $\Delta\bar{\lambda}$ = 0.25 nm. (b) NMT fitting with C_2-Swan-lsf data, inferred temperature from fixed line-width fitting: T = 5, 640 K.

The number of transitions in the range of 440 − 590 amount to well over one million for the ExoMol C_2 data base, or of the order of 100 times more transitions than those in the C_2-Swan line strength data. Table III illustrates the comparisons, and it also indicates that for Einstein A-coefficients larger than 103 s−1 there are of the order of 10 times more lines that are included in the ExoMol C_2database than that for C_2-Swan data.

Table 3. Number of transitions in the ranges 440 − 540 nm (16,950 − 22,725 cm−1)

Database Swan 440 − 590 nm	**440 − 590 nm**	**Acoeff > $10^3 S^{-1}$**
ExoMol C_2	1,251,235	169,566
C_2-Swan	17,689	17,689

Table IV displays agreements of lines within the indicated wave number range for oth- erwise the same identification for upper and lower levels of the transitions. Of the 169,566 ExoMol C_2 transitions, 16,988 or about ten per cent are within ten wave numbers of those listed in the 17,689 C_2-Swan data. However, only 3,123 of 169,566 transitions, or about 2%, are in agreement within the accuracy of 0.05 cm−1.

Table 4. Subset of the C_2 ExoMol data that agree within $\Delta\tilde{\nu}$ of 17,689 transitions in the C_2-Swan-lsf data in the range 440 − 590 nm (16,950 − 22,725 cm−1).

Database $\Delta\tilde{\nu} < 0.05\,\mathrm{cm}^{-1}$	$\Delta\tilde{\nu} < 0.2\,\mathrm{cm}^{-1}$	$\Delta\tilde{\nu} < 0.5\,\mathrm{cm}^{-1}$	$\Delta\tilde{\nu} < 2.0\,\mathrm{cm}^{-1}$	$\Delta\tilde{\nu} < 10.0\,\mathrm{cm}^{-1}$
ExoMol C_2 3,123	6,901	9,617	14,094	16,998

Laser-induced fluorescence and C_2-Swan Line Strengths

The C_2 line strength database has been extensively tested [11] including in the analysis of laser-plasma emission spectra. The use of accurate line strengths extends to analysis of LIF data [34] of the $\Delta v = 0$ sequence, and comparisons with Doppler-limited dye laser excitation spectra of the $\Delta v = +1$ C_2 Swan band [34, 35]. Figure 4 displays recorded and fitted LIF spectra of C_2 in the range of 507.723 − 516.696 nm. Analysis and fitting of laser induced fluorescence data requires knowledge of lower state wave numbers, and consequently a different script (not communicated here) as discussed in Ref. [7]. The laser step size in the experiment amounted to 0.002 cm−1 (0.05 picometer), and the full-width-half-maximum of the fitted spectrum amounts to 0.22 cm−1 (5.5 picometer) or about four times larger than the typical resolution of the C_2-Swan-lsf data.

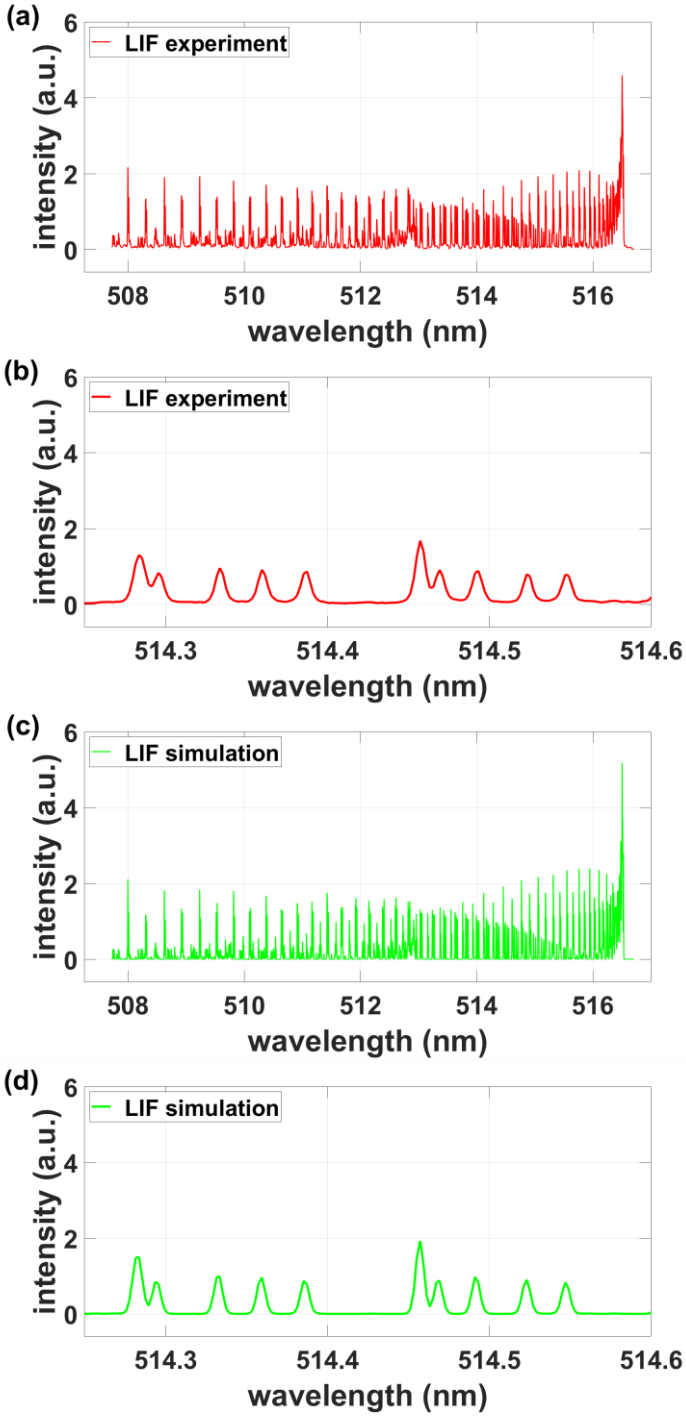

Figure 4. (a) Laser-induced fluorescence data, T = 2,716 K, laser step size: 0.00005 nm. (b) Expanded experiment data region. (c) Fitted data, T = 2,716 K, $\Delta^{-}\lambda$ = 0.0055 nm. (d) Expanded fitted data region.

Table 5. Number of transitions in the range 507.723 − 516.696 nm (19,354 − 19,696 cm−1).

Database Swan 507.723 − 516.696 nm	507.723 − 516.696 nm	Acoeff > 103s−1
ExoMol C_2	77,832	8,708
C_2-Swan	1,535	1,535

Table 6. Subset of the C_2 ExoMol data that agree within $\Delta\tilde{\nu}$ of 1,535 transitions in the C_2- Swan-lsf data in the range 507.723 − 516.696 nm (19,354 − 19,696 cm−1) .

Database $\Delta\tilde{\nu} < 0.05\,\mathrm{cm}^{-1}$	$\Delta\tilde{\nu} < 0.2\,\mathrm{cm}^{-1}$	$\Delta\tilde{\nu} < 0.5\,\mathrm{cm}^{-1}$
ExoMol C_2	651	1,194	1,337

4. Discussion

The agreement of the ExoMol C_2 and C_2-Swan-lsf databases line position is marginal when using accuracies of the order of 0.05 cm−1, or of the order of 1 picometer. For spectral resolutions of 10 cm−1, or about 0.25 nm, and for the $\Delta v = 0 \pm 1$ sequences and progressions, about 6% lower temperature is inferred when fitting 6,000 K, Exomol C_2 theory data with C_2-Swan-lsf data. Consequently, use of the C_2-Swan-lsf database is recommended. For measurements with spectral resolutions of 11.5 cm−1, or an average resolution of 0.35 nm, significant differences occur as well, namely, a 25 % lower temperature would be predicted when using the Exomol C_2 data base. The C_2-Swan-lsf line strength table is generated by fitting high resolution Fourier-transform data.

Wavelengths of individual positions should normally be predicted well in spectroscopy; however, there appear to be at least one order of magnitude differences in wavenumber predictions in the Exomol C_2 data base for a multitude of individual transitions within a molecular band. Hypothetical reasons for the apparent deficiency of the Exomol C_2 data base could be, for example, that the analysis using the measured active rotational-vibrational energy levels (MARVEL) procedure causes errors for generating line lists for ExoMol and/or that the selected spectroscopic model in ExoMol causes errors and/or that the predicted partition function in the Exomol C_2 data base introduces errors in the computation of molecular spectra.

References

1. Pretty W E 1927 Proc. Phys. Soc. 40 71
2. Johnson R C 1927 Phil. Trans. Royal Soc. A 226 157
3. Phillips J G and Davis S P 1968 The Berkeley Analysis of Molecular Spectra, Vol. 2, I. The Swan system of the C_2 molecule (Berkeley: Univ. California Press)
4. Parigger C G, Plemmons D H, Hornkohl J O, Lewis J W L 1994 J. Quant. Spectrosc. Radiat. Transf. 52 707
5. Dufour P, Blouin S, Coutu S, Fortin-Archambault M, Thibeault C, Bergeron P, Fontaine G, The Montreal White Dwarf Database: A Tool for the Community. In Astronomical Society of the Pacific (ASP) Conference Series 509, Proceedings of the 20th European White Dwarf workshop, Warwick, UK, 25–29 July 2016 ; Tremblay, P-E, Gaensicke B, Marsh T (Eds.) Utah Valley University: Orem, UT, USA, 2017; pp. 3–8. ISBN 978-1-58381-903-6. Available online: http://dev.montreal-whitedwarfdatabase.org (accessed on 11 May 2018).
6. Parigger C G, Helstern C M, Gautam G, and Drake D A 2019 J. Phys.: Conf. Ser. 1289 012001
7. Hornkohl J O, Nemes L, Parigger C G 2011 Spectroscopy of Carbon Containing Molecules, In: Nemes L and Irle S (Eds.) Spectroscopy, Dynamics and Molecular Theory of Carbon Plasmas and Vapors - Advances in the Understanding of the Most Complex High-Temperature Elemental System; Chap. 4, 113 – 166; (New Jersey: World Scientific)
8. Parigger C G 2023 Foundations 3 1
9. Parigger C G 2023 Preprints 2023 2023050423
10. Parigger C G and Hornkohl J O 2020 Quantum Mechanics of the Diatomic Molecule with Applications (Bristol: IOP Publishing)
11. Parigger C G and Hornkohl J O 2024 Quantum Mechanics of the Diatomic Molecule with Applications, 2nd edition (Bristol: IOP Publishing)
12. Tennyson J, Yurchenko S N, Al-Refaie A F, Clark V H J, Chubb K L, Conway E K, Dewan A, Gorman M N, Hill C, Lynas-Gray A E, Mellor T, McKemmish L K, Owens A, Polyansky O L, Semenov M, Somogyi N, Tinetti G, Upadhyay A, Waldmann I, Wang Y, Wright S, and Yurchenko O P 2020 J. Quant. Spectrosc. Radiat. Transf. 255 107228
13. Ochkin V N 2009 Spectroscopy of Low Temperature Plasma (Weinheim: Wiley-VCH)
14. Kunze H-J 2009 Introduction to Plasma Spectroscopy (Heidelberg: Springer)
15. Fujimoto T 2004 Plasma Spectroscopy (Oxford: Clarendon Press)
16. Demtr¨oder W 2014 Laser Spectroscopy 1: Basic Principles 5th ed. (Heidelberg: Springer)
17. Demtr¨oder W 2015 Laser Spectroscopy 2: Experimental Techniques 5th ed. (Heidelberg: Springer)

18. Miziolek A W, Palleschi V, Schechter I (Eds.) 2006 Laser Induced Breakdown Spectroscopy (LIBS): Fundamentals and Applications(New York: Cambridge Univ. Press)
19. Singh J P and Thakur S N (Eds.) 2020 Laser-Induced Breakdown Spectroscopy 2nd ed. (Am- sterdam: Elsevier)
20. Western C M 2017 J. Quant. Spectrosc. Radiat. Transf. 186 221
21. McKemmish L K 2021 WIREs Comput. Mol. Sci. 11 e1520
22. MATLAB Release 2022 R2022a Update 5 (Natik: The MathWorks, Inc.)
23. Nelder J A and Mead R A 1965 Comp. J. 7 308
24. Wigner E and Witmer E E 1928 Z. Phys. 51 859
25. Wigner E and Witmer E E 2000 On the structure of the spectra of two-atomic molecules according to quantum mechanics, In: Hettema H (Ed) Quantum Chemistry: Classic Scientific Papers 287 (Singapore: World Scientific: Singapore)
26. Yurchenko S N, Szabo I, Pyatenko E, Tennyson J 2018 Mon. Notices Royal Astron. Soc. 480 3397.
27. McKemmish L K, Syme A-M, Borsovszky J, Yurchenko S N, Tennyson J, Furtenbacher T, Cs´asz´ar A G 2020 Mon. Notices Royal Astron. Soc. 497 1081
28. Parigger C G 2023 Atoms 11 62
29. Condon E U and Shortley G H 1964 The Theory of Atomic Spectra (Cambridge: Cambridge Univ Press)
30. Hilborn R C 1982 Am. J. Phys. 50 982
31. Thorne A P 1988 Spectrophysics 2nd ed. (New York: Chapman and Hall)
32. Ciddor P E 1996 Appl. Opt. 35 1567
33. Corney A C 1977 Atomic and Laser Spectroscopy (Oxford: Clarendon Press)
34. Hornkohl J O, Parigger C G, Lewis J W L 1996 On the Use of Line Strengths in Applied Diatomic Spectroscopy, In: Technical Digest Series (Optica Publishing Group, 1996) of the Laser Applications to Chemical and Environmental Analysis Conference, Orlando, FL, USA, 20-22 March 1996, paper LThD 16.
35. Suzuki T, Saito S, Hirota E 1985 J. Molec. Spectrosc. 113 399